Werk

Jahr: 1975
Kollektion: fid.geo
Signatur: 8 Z NAT 2148:41
Digitalisiert: Niedersächsische Staats- und Universitätsbibliothek Göttingen
Werk Id: PPN1015067948_0041
PURL: http://resolver.sub.uni-goettingen.de/purl?PPN1015067948_0041

LOG Id: LOG_0011
LOG Titel: Statistical behaviour of elastic waves in a reverberating solid
LOG Typ: article

Übergeordnetes Werk

Werk Id: PPN1015067948
PURL: http://resolver.sub.uni-goettingen.de/purl?PPN1015067948
OPAC: http://opac.sub.uni-goettingen.de/DB=1/PPN?PPN=1015067948

Contact

Niedersächsische Staats- und Universitätsbibliothek Göttingen
Georg-August-Universität Göttingen
Platz der Göttinger Sieben 1
37073 Göttingen
Germany
Email: gdz@sub.uni-goettingen.de

J. Geophys. 41, 1–12, 1975

Original Investigations

Statistical Behaviour of Elastic Waves in a Reverberating Solid

J. Drisler and P. Antony-Spies

Institute of Meteorology and Geophysics,
University Frankfurt am Main

Received May 3, 1974

Abstract. A reverberation method of measuring the Q-value of a rock sample of arbitrary size and shape is investigated theoretically on the basis of randomly travelling shear and compressional waves. Formulae are derived for the mean attenuation of these waves, their energy ratios and the energy conversion rates of the two types into each other. The evaluation for a spherical sample with an isotropic and a sine distribution of the wave intensity incident on the sample surface gives energy ratios E_P/E_S between 0.35 and 0.60 depending on the wave velocities. The influence of size and shape of the sample is found to be rather weak generally for typical laboratory samples with dimensions from about 2 to 20 cm.

Key words: Elastic Waves-Attenuation — Q-value — Reverberation — Energy-Statistics — Wave Conversion — Wave Mixture.

1. Introduction

One of the most striking results of the first seismic experiments on the moon was the discovery that elastic waves have an extremely small attenuation compared with the values obtained for the solid earth. Therefore much work has been done in the last few years in order to find out the reasons. Most of the investigations were laboratory measurements of elastic wave absorption in rock under various lunar environmental conditions.

In this paper we want to point out some interesting theoretical aspects of the absorption measurements of Herminghaus and Berckhemer (1974). They applied the reverberation techniques well known in architectural acoustics using a rock sample as the reverberation chamber. Applications to ultrasonic absorption measurements in liquids are described by Kurtze and Tamm (1953), Bergmann (1954) and Ohsawa and Wada (1967). Reverberation is the persistence of sound in an enclosure as the result of continuous reflections at the walls after the sound source has been turned off. The sample surface which is usually irregular and other inhomogeneities serve as reflective sources and cause the sound energy distribution to become uniform. The reverberation time at a specific frequency is a reciprocal measure for the absorption and proportional to the Q-value of the sample.

There are two important features which distinguish the reverberation method applied to solid samples from its analogue in architectural acoustics. First, in addition to compressional waves also shear waves have to be considered and second, the measured attenuation is taken to be a characteristic material property and should be independent of the shape and the size of the sample. The difference between the present method and the conventional methods of elastic wave absorption measurements (Truell *et al.*, 1969) is, that in the latter scattering by inhomogeneities and reflections by surface irregularities must be prevented with the aid of adequately chosen samples and high precision mechanical surface preparation. In the present method the samples are not mechanically prepared. Apart from the practical advantage of this, the method simulates another important discovery in lunar seismograms: the strong multiple scattering and randomness of reflections of seismic waves. The results of our investigations might be applied in principle to other large scale multiple scattering and random reflection phenomena in seismology.

2. *Physical Model*

The problem is to describe the mean time behaviour of the elastic wave energy in a solid after a single pulse has been transmitted from a point source on the surface of the sample. The solution presented below is a statistical approach based on the following assumptions:

(1) The elastic wave energy is described by randomly travelling shear and compressional waves (S and P waves).

(2) The mean energy E_{PS} of S waves generated per unit time by P waves incident on the surface and on inhomogeneities is proportional to the total P wave energy E_P. The same is assumed for the mean energy E_{SP} of P waves generated by S waves. We write

$$E_{PS} = A \cdot E_P, \tag{1}$$

$$E_{SP} = B \cdot E_S , \tag{2}$$

where the factors A and B are independent of time.

The quantities E_{PS} and E_{SP} will be called "*P/S and S/P energy conversion rates*" respectively, and the factors A and B "*relative energy conversion rates*". The latter account for the material and the geometrical properties of the sample.

For illustration we use a simple ray model for a homogeneous sample. Consider a single ray from a compressional pulse emitted from the source at the time $t=0$. At the first reflection from the surface it splits up into a P

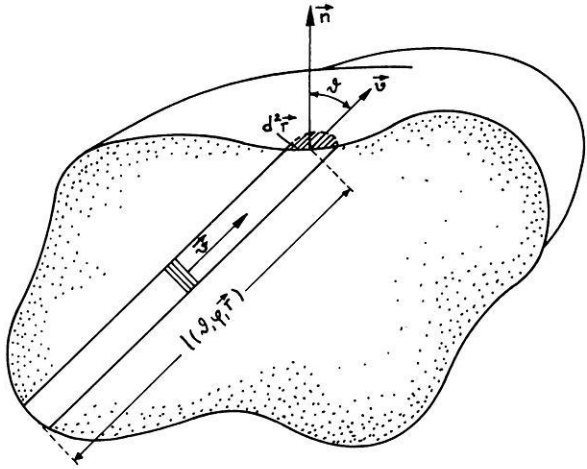

Fig. 1. Cut of the sample in the plane of incidence of an elastic wave. The azimuth φ is the angle between the cut and any reference plane containing the normal vector $\vec{n}$

and an S ray. Each of them splits up again at the second and all subsequent reflections. After n reflections there are 2^n P and S rays. At a given time t we have

$$n \approx \frac{\bar{v}}{\bar{l}}\, t\,, \tag{3}$$

where $\bar{l}$ is the mean free path and $\bar{v}$ the mean velocity of the rays. For samples with a diameter of about 10 cm the mean number of reflections $\bar{l}/\bar{v}$ suffered per second by a ray lies between 10^4 and 10^5. The number of rays increases very rapidly with time causing a corresponding fine spatial distribution of energy and an equilibrium mixture of P and S waves.

3. P/S and S/P Energy Conversion Rates

In order to calculate the energy conversion rates we use the simple model of the last section. We define local angular distribution functions $f_{\mathrm{P}}(\vartheta, \varphi, \vec{r})$ and $f_{\mathrm{S}}(\vartheta, \varphi, \psi, \vec{r})$ of mean P and S wave energy flux as follows: Consider the energy $d\varepsilon_{\mathrm{P}}$ of P waves travelling in the direction ϑ, φ towards the surface element $d^2\vec{r}$ at the point $\vec{r}$ (Fig. 1). It is contained in a thin prism of length $l(\vartheta, \varphi, \vec{r})$. The time it takes P waves with velocity v_{P} to pass the prism is the ratio $l(\vartheta, \varphi, \vec{r}) / v_{\mathrm{P}}$. Denoting the mean intensity of P waves by $I_{\mathrm{P}}(\vartheta, \varphi, \vec{r})$ and the solid angle by $d\Omega = \sin\vartheta\, d\vartheta\, d\varphi$, we have

$$d\varepsilon_{\mathrm{P}} = I_{\mathrm{P}}(\vartheta, \varphi, \vec{r})\, \frac{l(\vartheta, \varphi, \vec{r})}{v_{\mathrm{P}}} \cos\vartheta\, d^2\vec{r}\, d\Omega\,. \tag{4}$$

For S waves the analogous expression is

$$d\varepsilon_S = I_S(\vartheta, \varphi, \psi, \vec{r}) \frac{l(\vartheta, \varphi, \vec{r})}{v_S} \cos\vartheta d^2\vec{r} d\Omega d\psi , \tag{5}$$

where the angle ψ describes the polarization such that $\psi = 0$ for SV waves and $\psi = \pi/2$ for SH waves. The total P and S wave energies E_P and E_S in the sample are obtained by integration:

$$E_P = \int I_P(\vartheta, \varphi, \vec{r}) \frac{l(\vartheta, \varphi, \vec{r})}{v_P} \cos\vartheta d^2\vec{r} d\Omega \tag{6}$$

and

$$E_S = \int I_S(\vartheta, \varphi, \psi, \vec{r}) \frac{l(\vartheta, \varphi, \vec{r})}{v_S} \cos\vartheta d^2\vec{r} d\Omega d\psi . \tag{7}$$

The local angular distribution functions of the energy flux towards the surface can then be defined by

$$f_P(\vartheta, \varphi, \vec{r}) \equiv \frac{1}{E_P} I_P(\vartheta, \varphi, \vec{r}) \frac{l(\vartheta, \varphi, \vec{r})}{v_P} \cos\vartheta \tag{8}$$

and

$$f_S(\vartheta, \varphi, \psi, \vec{r}) \equiv \frac{1}{E_S} I_S(\vartheta, \varphi, \psi, \vec{r}) \frac{l(\vartheta, \varphi, \vec{r})}{v_S} \cos\vartheta . \tag{9}$$

They are normalized to 1 according to Eqs. (6) and (7). Expressing the P/S and S/P energy conversion rates in terms of these functions we have

$$\begin{aligned} E_{PS} &= \int A_{PS}(\vartheta, \varphi) I_P(\vartheta, \varphi, \vec{r}) \cos\vartheta d^2\vec{r} d\Omega \\ &= E_P v_P \int A_{PS}(\vartheta, \varphi) \frac{f_P(\vartheta, \varphi, \vec{r})}{l(\vartheta, \varphi, \vec{r})} d^2\vec{r} d\Omega = E_P A \end{aligned} \tag{10}$$

and

$$E_{SP} = E_S v_S \int A_{SP}(\vartheta, \varphi, \psi) \frac{f_S(\vartheta, \varphi, \psi, \vec{r})}{l(\vartheta, \varphi, \vec{r})} d^2\vec{r} d\Omega d\psi \equiv E_S B , \tag{11}$$

where $A_{PS}(\vartheta, \varphi)$ and $A_{SP}(\vartheta, \varphi, \psi)$ are the ratios of the S wave energy generated at a surface element to the energy of P waves incident in the direction ϑ, φ and vice versa.

In the case of incident S waves only the component in the plane of incidence is converted. We can therefore write

$$A_{SP}(\vartheta, \varphi, \psi) = A_{SP}(\vartheta, \varphi) \cdot \cos^2 \psi , \tag{12}$$

where $A_{SP}(\vartheta, \varphi)$ refers to incident S waves without regard to polarization.

According to their general form the expressions (10) and (11) are supposed to be valid also for models of scattering and diffraction including wave theory instead of simple rays. We note by inspection of the integrals that the energy conversion rates generally depend on size and shape of the sample.

The practical calculation of the relative energy conversion rates A and B from the formulas (10) and (11) requires special assumptions about the angular distribution functions. In the two following examples the sample has been chosen to be a sphere with radius R. In model I we assume the elastic wave intensity to be homogeneous and isotropic:

$$\begin{aligned} f_P(\vartheta, \varphi, \vec{r}) &= \frac{1}{8\pi^2 R^2} , \\ f_S(\vartheta, \varphi, \psi, \vec{r}) &= \frac{1}{8\pi^3 R^2} . \end{aligned} \tag{13}$$

In model II a cosine distribution is assumed:

$$\begin{aligned} f_P(\vartheta, \varphi, \vec{r}) &= \frac{1}{4\pi^2 R^2} \cos\vartheta , \\ f_S(\vartheta, \varphi, \psi, \vec{r}) &= \frac{1}{4\pi^3 R^2} \cos\vartheta . \end{aligned} \tag{14}$$

The S wave intensity is independent of polarisation in both models. The energy ratios A_{PS} and A_{SP} are given in plane wave theory by the expressions (Gutenberg, 1944):

$$A_{PS}(\vartheta) = \frac{4 L_P^2}{(L_P^2 + 1)^2} \tag{15}$$

and

$$A_{SP}(\vartheta) = \frac{4 L_S^2}{(L_S^2 + 1)^2} , \tag{16}$$

where

$$L_P^2 = \frac{\left[\left(\frac{v_P}{v_S}\right)^2 - 2\sin^2\vartheta\right]^2}{2\sin\vartheta\sin 2\vartheta\sqrt{\left(\frac{v_P}{v_S}\right)^2 - \sin^2\vartheta}} \tag{17}$$

and

$$L_S^2 = \left(\frac{v_P}{v_S}\right)^2 \frac{\cot 2\vartheta\cos 2\vartheta}{2\sin\vartheta\sqrt{\left(\frac{v_S}{v_P}\right)^2 - \sin^2\vartheta}} \tag{18}$$

They are plotted in Fig. 2 for different ratios of the wave velocities. The relative energy conversion rates have been listed in Table 1. We observe that the values are strongly effected by the angular distribution functions of the incident energy. They are greater for model I than for model II because the mean distance between two reflections is longer in model II. The influence of the velocity ratio is comparably weak.

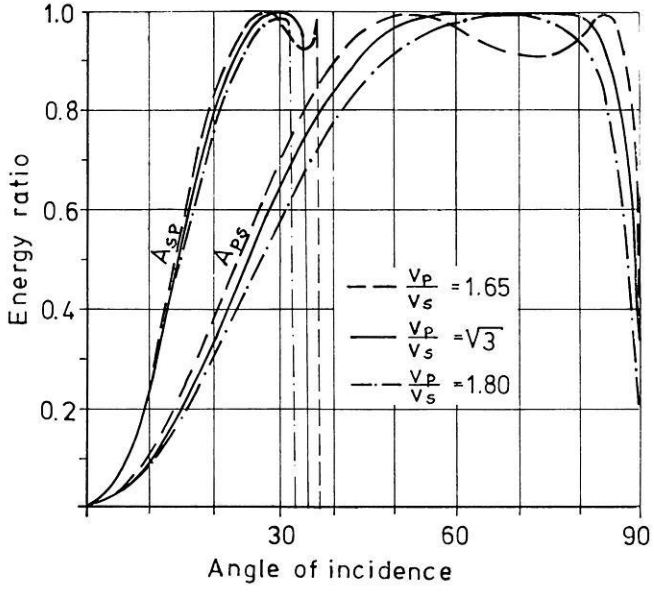

Fig. 2. Energy ratios of reflected P waves to incident S waves and vice versa as a function of the angle of incidence for various velocity ratios v_P/v_S. (after Gutenberg)

Table 1. Relative energy conversion rates A and B for various ratios v_P/v_S

model	v_P / v_S	$A \cdot \frac{R}{v_P}$	$B \cdot \frac{R}{v_S}$
I	1.65	2.04	1.68
II		0.72	0.50
I	$\sqrt{3}$	1.78	1.69
II		0.83	0.50
I	1.80	1.57	1.69
II		0.79	0.50

4. *Damping of P and S Wave Mixtures*

We shall now calculate the time dependence of elastic wave energy. The change of P wave energy in time is given by the energy increase E_{SP} per unit time by S/P conversion, the decreases $-E_{PS}$ by P/S conversion and $-D_P$ by attenuation

$$\frac{dE_P}{dt} = E_{SP} - E_{PS} - D_P \,. \tag{19}$$

For S waves we have

$$\frac{dE_S}{dt} = -E_{SP} + E_{PS} - D_S \,. \tag{20}$$

The energy losses D_P and D_S per unit time can be expressed in terms of the energy damping constants a and b

$$D_P = a \cdot E_P \,, \tag{21}$$

$$D_S = b \cdot E_S \,. \tag{22}$$

The damping constants are closely related to the well known Q-value of elastic waves defined by

$$\frac{1}{Q} = \frac{1}{2\pi} \frac{\Delta E}{E} \,, \tag{23}$$

where $\Delta E/E$ is the relative energy loss per cycle. Division of the absolute energy loss per cycle, ΔE, by the period T gives

$$D_P = \frac{\Delta E_P}{T} = \frac{2\pi}{Q_P T} E_P \equiv a E_P , \tag{24}$$

$$D_S = \frac{\Delta E_S}{T} = \frac{2\pi}{Q_S T} E_S \equiv b E_S . \tag{25}$$

Inserting the expressions for D_P, D_S, E_{PS} and E_{SP} into Eqs. (19) and (20) we obtain two coupled linear differential equations of first order in time:

$$\frac{dE_P}{dt} = E_P(-A-a) + E_S B, \tag{26}$$

$$\frac{dE_S}{dt} = E_P A + E_S(-B-b) . \tag{27}$$

They are solved by letting

$$E_P = E_{P0} \cdot e^{-ct} , \tag{28}$$

$$E_S = E_{S0} \cdot e^{-ct} , \tag{29}$$

where the constant c is given by

$$c = \frac{A+B+a+b}{2} - \sqrt{\frac{(A+B+a+b)^2}{4} - Ab - aB - ab} . \tag{30}$$

The solution shows that the decreases of the total P and S wave energies within the solid are the same, giving a constant ratio E_P/E_S.

By inserting the solutions (28) and (29) into the differential Eqs. (26) and (27) we obtain

$$\frac{E_P}{E_S} = \frac{E_{P0}}{E_{S0}} = \frac{B}{c+A+a} = \frac{c+B+b}{A} . \tag{31}$$

If the damping of P and S waves is sufficiently small the energy ratio only depends on the relative energy conversion rates:

$$\frac{E_P}{E_S} = \frac{B}{A} . \tag{32}$$

Some numerical values of E_P/E_S for the two models in the last section are given in Table 2. We note that the energy of S waves is greater than the P wave energy approximately by a factor of 2.

Table 2. Ratio of P wave to S wave energy for vanishing absorption for various ratios v_P/v_S

model	v_P / v_S	$E_P / E_S = B / A$
I	1.65	0.50
II		0.42
I	$\sqrt{3}$	0.55
II		0.35
I	1.80	0.60
II		0.35

5. *Discussion*

The previous considerations yield the theoretical background for the absorption measurements of Herminghaus and Berckhemer (1974). The quantity determined by the experiments is the mixed damping constant c. According to equation (30) it can be calculated from the damping constants a and b of pure P and S waves and the relative energy conversion rates A and B. The evaluation for a typical case of the ratio a/b is shown in Fig. 3, where the mixed damping constant is plotted against the relative energy conversion rates. For convenience the dimensionless quantities c/a, A/a, B/a and a/b are used. In Fig. 4 we have plotted the curves of constant mixed damping in the $A/a - B/a$ plane. Here the straight isolines confirm the simplicity of the relations. The mixed damping always lies between the individual damping constants. It approaches the S wave damping if the relative conversion rate A of P into S waves is high in comparison with the reverse process and vice versa.

As mentioned before the mixed damping is effected in general by the shape and the size of the sample. Because of the integrals in Eqs. (10) and (11) the influence of the shape is not sufficiently transparent for straightforward considerations. The effect of the size of the sample, however, can be easily seen. Let the relative conversion rates of a reference sample be A_0 and B_0. The free path of the rays be $l_0(\vartheta, \varphi, \vec{r})$. For a body with the same shape but a different size all lengths are multiplied by a constant δ:

$$l(\vartheta, \varphi, \vec{r}) = \delta \cdot l_0(\vartheta, \varphi, \vec{r}) . \tag{33}$$

The relative conversion rates are

$$A(\delta) = \frac{1}{\delta} A_0$$

and (34)

$$B(\delta) = \frac{1}{\delta} B_0 .$$

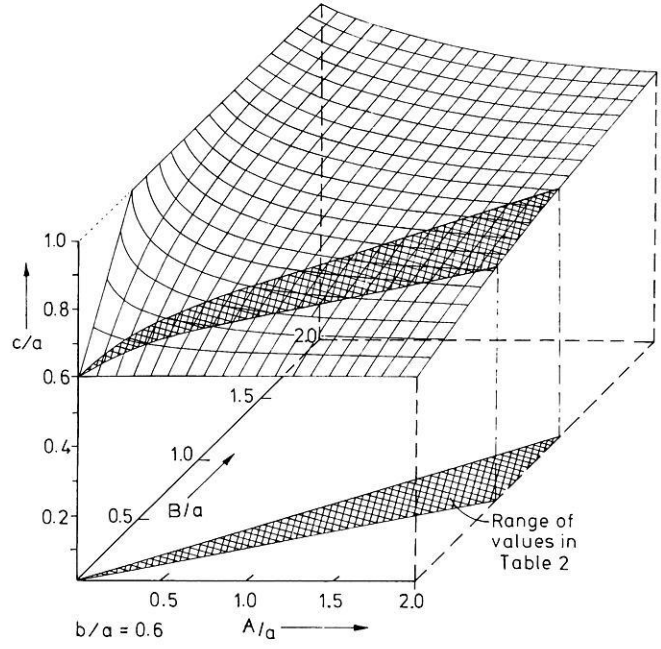

Fig. 3. Mixed damping versus the two relative energy conversion rates with the fixed ratio b/a of the damping constants due to pure S and P waves

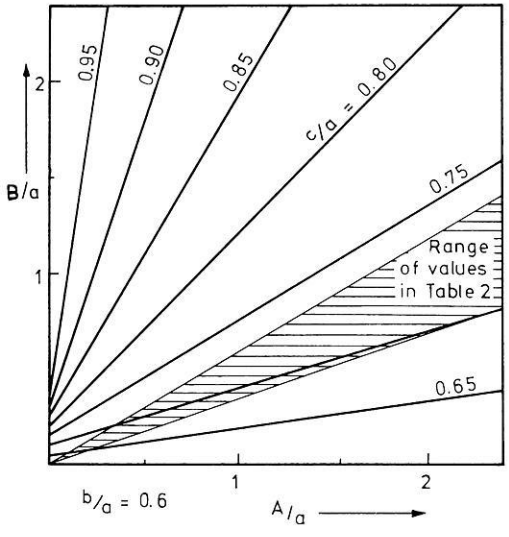

Fig. 4. Lines of constant mixed damping for variable relative energy conversion rates

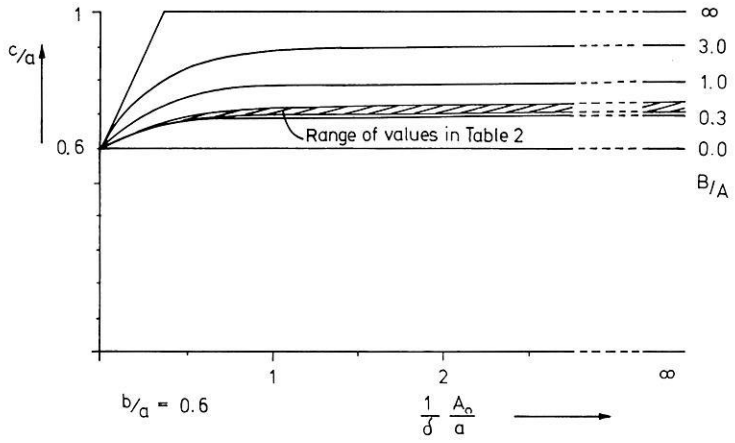

Fig. 5. Dependence of the mixed damping on the size parameter δ of the sample. The conversion rate of the reference sample is denoted by A_0

For a fixed shape which means a constant ratio B/A we get a straight line with the slope B_0/A_0 through the origin in the $A/a - B/a$ plane in Figs. 3 and 4. Inserting Eqs. (34) into the formula (30) we obtain the mixed damping as a function of the size parameter δ. It is plotted in Fig. 5 versus the quantity $A/a = A_0/a\delta$ for $b/a = 0.6$ and various shape parameters B_0/A_0. There are two limiting cases. For large bodies ($\delta \gg A/a$) the conversion rates are low and the mixed damping is near the weaker damping constant. For small bodies the conversion rates become high and the mixed damping is independent of size. Obviously this is achieved if

$$A_0/a\delta > 1.5 \,. \tag{35}$$

In the experiments of Herminghaus and Berckhemer (1974) the samples had diameters of $d = 5$ to 10 cm. The measured Q-values are in the range of 100 to 800 for frequencies between 100 and 400 kHz. The P wave velocities v_P are between 2500 and 5000 m/s. Taking the most unfavourable data from the measurements and from Table 1 for a reference sample ($\delta = 1$) we have, using Eq. (24):

$$\frac{A_0}{c} = A_0 \frac{Q\,T}{2\,\pi} \gtrsim 100 \,.$$

If we assume that $a < 5c$ we can be sure that the mixed damping measured by the reverberation method is independent of the size.

As shown by Fig. 5 the dependence on the shape is also weak, supposed that the estimates of the models I and II are realistic. This might be the case if there are no extreme deviations from a spherical shape like long

rods for example. Small shape variations are thought to be simulated to a certain amount by variation of the angular distribution functions.

Finally, we can give a rule for mixing the Q-values of pure P and S waves. From Eqs. (23) to (25) one obtains

$$\frac{1}{Q} = \frac{1}{Q_P} \frac{E_P}{E_P + E_S} + \frac{1}{Q_S} \frac{E_S}{E_P + E_S}, \tag{36}$$

giving for our special models a mixing rule:

$$\frac{1}{Q} = \alpha \frac{1}{Q_P} + (1 - \alpha) \frac{1}{Q_S}, \; \alpha = 0.68 \pm 0.06. \tag{37}$$

For bodies larger than laboratory samples like regions of the seismic wave scattering in the outer layers of the moon fixed numbers of α might become questionable. However, one should be able to give a range of the mixed damping reaching from slightly above the smaller component to a certain considerable amount below the greater one.

Acknowledgements. The authors would like to express their appreciation to Prof. Dr. H. Berckhemer for suggesting this problem. They thank him, Prof. Dr. W. Jacoby and Ch. Herminghaus for various helpful discussions. This work was supported by the Bundesministerium für Bildung und Wissenschaft under contract no. WRK 246 and by the Deutsche Forschungsgemeinschaft under contract no. 299/36.

References

Bergmann, L.: Der Ultraschall und seine Anwendung in Wissenschaft und Technik, 6th ed., Stuttgart: S. Hirzel 1954

Gutenberg, B.: Energy ratio of reflected and refracted seismic waves. Bull. Seism. Soc. Am. *34*, 85–101, 1944

Herminghaus, Ch., Berckhemer, H.: Ultrasound absorption measurements in rock samples at low temperatures. J. Geophys. *40*, 341–354, 1974

Kurtze, G., Tamm, K.: Measurements of sound absorption in water and aqueous solutions of electrolytes. Acoustica *3*, 33–48, 1953

Ohsawa, T., Wada, Y.: Resonance reverberation method of ultrasonic measurements of liquids from 10 to 300 kc. Jap. J. Appl. Phys. *6*, 1351–1356 1967

Truell, R., Elbaum, Ch., Chick, B.: Ultrasonic methods in solid state physics. New York: Academic Press 1969

Jürgen Drisler
Peter Antony-Spies
Institut für Meteorologie
und Geophysik der Universität
D-6000 Frankfurt am Main
Feldbergstraße 47
Federal Republic of Germany